International Journal of Theoretical Physics, Vol. 33, No. 3, 1994

Qualitative Analysis of a Class of Bianchi VI_0 Imperfect Fluid Cosmologies

G. Abolghasem[1] and A. A. Coley[1]

Received August 13, 1993

A set of "dimensionless" equations of state is used to show that the Einstein field equations governing a class of Bianchi VI_0 imperfect fluid cosmologies reduce to a plane-autonomous system of equations. The qualitative behavior of the underlying cosmological models is obtained by investigating this plane-autonomous system.

1. INTRODUCTION

Bianchi cosmologies, as alternatives to standard perfect fluid Friedmann–Robertson–Walker (FRW) models, are of interest because of their richer structures, both geometrically and physically. Bianchi VI_0 spatially homogeneous models are of interest because they are complex enough to allow the inclusion of heat conduction in a natural way. The role played by viscosity and dissipative processes in cosmology has already attracted much attention, since it provides a possible explanation for both the currently observed highly isotropic matter distribution and the high entropy per baryon in the present state of the universe (Misner, 1968). The influence of viscosity on the character of cosmological evolution has been studied by many other researchers. Belinskii and Khalatnikov (1976) were the first to consider the qualitative behavior of spatially homogeneous viscous fluid cosmological models in any generality. Models which include heat conduction have also been studied in spatially homogeneous cosmologies (Bradley and Sviestins, 1984).

In some recent papers, Bianchi V imperfect fluid cosmology was investigated (Coley, 1990*a*). The Einstein field equations governing these

[1]Department of Mathematics, Statistics and Computing Science, Dalhousie University, Halifax, Nova Scotia, Canada B3H 3J5.

0020-7748/94/0300-0695$07.00/0

cosmological models reduce to a plane-autonomous system of equations upon the introduction of a set of "dimensionless" equations of state (Coley, 1990*b*), thus enabling a qualitative analysis of the models to be undertaken (Coley and Dunn, 1992). The purpose of this work is to use the above approach to study the qualitative behavior of a class of Bianchi VI_0 spatially homogeneous cosmologies in which the source of the gravitational field is an imperfect fluid with both viscosity and heat conduction.

2. EINSTEIN FIELD EQUATIONS

The diagonal Bianchi type VI_0 spatially homogeneous metric is given by

$$ds^2 = -dt^2 + X^2(t)\,dx^2 + Y^2(t)e^{-2x}\,dy^2 + Z^2(t)e^{2x}\,dz^2 \tag{2.1}$$

in which the source of the gravitational field is taken to be a (comoving) viscous fluid with heat conduction, with energy-momentum tensor

$$T_{ab} = (\rho + \bar{p})u_a u_b + \bar{p}g_{ab} - 2\eta\sigma_{ab} + q_a u_b + u_a q_b \tag{2.2}$$

where

$$\bar{p} = p - \zeta\theta \tag{2.3}$$

where ρ is the matter density, σ_{ab} is the shear tensor, q_a is the heat conduction vector and orthogonal to the fluid four-velocity u^a, p is the thermodynamic pressure, θ is the expansion scalar, and ζ and η are the coefficients of bulk and shear viscosity, respectively. The nontrivial Einstein field equations are given by

$$\frac{\dot{X}\dot{Y}}{XY} + \frac{\dot{X}\dot{Z}}{XZ} + \frac{\dot{Y}\dot{Z}}{YZ} - \frac{1}{X^2} = \rho \tag{2.4}$$

$$\frac{\dot{Z}}{Z} - \frac{\dot{Y}}{Y} = q_1 \tag{2.5}$$

$$-\frac{\ddot{Y}}{Y} - \frac{\ddot{Z}}{Z} - \frac{\dot{Y}\dot{Z}}{YZ} - \frac{1}{X^2} = \bar{p} - \frac{2}{3}\eta\left(2\frac{\dot{X}}{X} - \frac{\dot{Y}}{Y} - \frac{\dot{Z}}{Z}\right) \tag{2.6}$$

$$-\frac{\ddot{X}}{X} - \frac{\ddot{Z}}{Z} - \frac{\dot{X}\dot{Z}}{XZ} + \frac{1}{X^2} = \bar{p} - \frac{2}{3}\eta\left(2\frac{\dot{Y}}{Y} - \frac{\dot{X}}{X} - \frac{\dot{Z}}{Z}\right) \tag{2.7}$$

$$-\frac{\ddot{X}}{X} - \frac{\ddot{Y}}{Y} - \frac{\dot{X}\dot{Y}}{XY} + \frac{1}{X^2} = \bar{p} - \frac{2}{3}\eta\left(2\frac{\dot{Z}}{Z} - \frac{\dot{X}}{X} - \frac{\dot{Y}}{Y}\right) \tag{2.8}$$

where the units have been chosen such that $8\pi G = 1$. We regard (2.4) as the definition of ρ. Note that when $Y/Z = \text{const}$, the heat conduction is zero. For the Bianchi VI_0 models under consideration, the shear scalar, expan-

sion, and the Ricci curvature of the three-dimensional hypersurfaces of homogeneity, ${}^3R$, are given by

$$\sigma^2 = \frac{1}{3}\left[\left(\frac{\dot{X}}{X}\right)^2 + \left(\frac{\dot{Y}}{Y}\right)^2 + \left(\frac{\dot{Z}}{Z}\right)^2 - \frac{\dot{X}\dot{Y}}{XY} - \frac{\dot{Y}\dot{Z}}{YZ} - \frac{\dot{X}\dot{Z}}{XZ}\right] \tag{2.9}$$

$$\theta = \frac{\dot{X}}{X} + \frac{\dot{Y}}{Y} + \frac{\dot{Z}}{Z} \tag{2.10}$$

$${}^3R = -6X^{-2} \tag{2.11}$$

By (2.4), (2.9), and (2.10), we obtain the "generalized Friedmann equation" or "first integral"

$$\theta^2 = \frac{3}{X^2} + 3\sigma^2 + 3\rho \tag{2.12}$$

and by adding (2.6)–(2.8) we obtain the Raychaudhuri equation

$$\dot{\theta} = -\frac{1}{3}\theta^2 - 2\sigma^2 - \frac{1}{2}(\rho + 3\bar{p}) \tag{2.13}$$

By taking the derivative of (2.12) and using (2.6), (2.7), and (2.5), we obtain the independent equation

$$\dot{\sigma} = -2\eta\sigma - \sigma\theta + \frac{1}{\sqrt{3}}\left(4 - \frac{q_1^2}{\sigma^2}\right)^{1/2}\left(\frac{1}{3}\theta^2 - \sigma^2 - \rho\right) \tag{2.14}$$

Finally, from the conservation law ($T^{ab}{}_{;b}u_a = 0$) we find that

$$\dot{\rho} = -(\rho + p)\theta + \zeta\theta^2 + 4\eta\sigma^2 \tag{2.15}$$

Now, we define the variables β and x by

$$\beta = 2\sqrt{3}\frac{\sigma}{\theta} \tag{2.16}$$

(which measures the rate of shear in terms of the expansion), and

$$x = \frac{3\rho}{\theta^2} \tag{2.17}$$

(which measures the dynamical importance of the matter content). We also introduce a new time coordinate Ω by

$$l = e^{-\Omega}; \qquad \frac{d\Omega}{dt} = -\frac{\theta}{3} \tag{2.18}$$

(where l is the representative length scale with $\theta = 3\dot{l}/l$). Then with the aid of (2.12) and (2.13), equations (2.14) and (2.15) reduce to

$$\frac{d\beta}{d\Omega} = \frac{1}{2}\beta\left(4 - \beta^2 - x - \frac{9p}{\theta^2} + \frac{9\zeta}{\theta} + \frac{12\eta}{\theta}\right) - \frac{1}{2}\left(4 - \frac{q_1^2}{\sigma^2}\right)^{1/2}(4 - \beta^2 - 4x) \tag{2.19}$$

$$\frac{dx}{d\Omega} = x(1 - x - \beta^2) + \frac{9p}{\theta^2}(1 - x) - \frac{9\zeta}{\theta}(1 - x) - \frac{3\eta}{\theta}\beta^2 \tag{2.20}$$

Finally, from (2.12) and the nonnegative nature of ρ, we observe that the region of interest is

$$\begin{aligned} \beta^2 + 4x &\leq 4 \\ x &\geq 0 \end{aligned} \tag{2.21}$$

3. EQUATIONS OF STATE

Now, in order to complete the system of equations we need to specify four equations of state for p, ζ, η, and q_1. Following Coley (1990*b*), we introduce "dimensionless" equations of state of the following form:

$$\begin{aligned} p/\theta^2 &= \tfrac{1}{3}(\gamma - 1)x \\ \zeta/\theta &= \zeta_0 x^m \\ \eta/\theta &= \eta_0 x^n \\ q_1/\theta &= (1/\sqrt{3})\kappa_0\beta \end{aligned} \tag{3.1}$$

The first equation is the barotropic equation of state, $p = (\gamma - 1)\rho$, where $1 \leq \gamma \leq 2$. The other three equations are assumed so that (2.19) and (2.20) reduce to a plane-autonomous system [where ζ_0, η_0, and κ_0 ($0 \leq \kappa_0 \leq 1$) are nonnegative constants and m and n are also nonnegative constant parameters]. Here we shall simply remark that equations (3.1) are assumed to be valid (at least) in an asymptotic sense. In contrast to the work of Coley and Dunn (1992), we have included heat conduction in a general way. The quantity q_1 appears in our plane-autonomous system, so that it is necessary to extend the set of "dimensionless equations of state" to incorporate a dimensionless equation of state for q_1 [see the last equation of (3.1)] in order to keep the system two-dimensional and autonomous. In principle, we consider $q_1/\theta = f(x, \beta)$, but for simplicity we choose f to be a function of only β. This equation of state includes an adjustable parameter κ_0, so that heat conduction can be "turned off." By using these equations of state, the Einstein field equations (2.19) and (2.20) for a Bianchi type VI_0 spatially homogeneous viscous fluid model with heat

conduction reduce to the following plane-autonomous system:

$$\frac{d\beta}{d\Omega} = \frac{1}{2}\beta[4 - \beta^2 - (3\gamma - 2)x + 9\zeta_0 x^m + 12\eta_0 x^n] - (1 - \kappa_0^2)^{1/2}(4 - \beta^2 - 4x) \tag{3.2}$$

$$\frac{dx}{d\Omega} = x[(3\gamma - 2)(1 - x) - \beta^2] - 9\zeta_0 x^m(1 - x) - 3\eta_0 x^n\beta^2 \tag{3.3}$$

In the next section, we shall analyze the above system using techniques employed in Collins (1971), Belinskii and Khalatnikov (1976), and Coley and Dunn (1992). The remaining sections will be devoted to the results of the analysis.

4. QUALITATIVE BEHAVIOR OF SOLUTION

The region of interest $\mathscr{R}$ defined by (2.21) is the region bounded by the parabola $\beta^2 + 4x = 4$ and the β axis. The positive and negative arms of the parabola from $(1, 0)$ to $(0, 2)$ and $(0, -2)$, respectively, are themselves trajectories. In most cases we will see that the β axis from $(0, 0)$ to $(0, -2)$ and $(0, 2)$ is itself a trajectory. We shall also see that in general there will be at most seven isolated singular points in $\mathscr{R}$, but not all occur at the same time. They are as follows:

$$(0, 0), (0, 2), (0, -2), (0, 2\Delta), (\Sigma, 0), (1, 0), (\bar{x}, \bar{\beta})$$

where Σ, Δ, $\bar{x}$, and $\bar{\beta}/2$, all belonging to the interval $(0, 1)$, will be defined below.

The analysis then consists of determining the nature of these singular points (and calculating the associated eigenvectors). We shall describe a number of cases and display their phase diagrams in the figures. We have generally chosen to consider $m = n$ in each case below. In addition, we have considered $m = n = 1/2$ and $m = n = 3/2$ as representative of the cases $0 < m, n < 1$, and $m, n > 1$, respectively. In the figures arrows refer to evolution in Ω-time ($\Omega \to \infty$ indicates $t \to 0$).

(*a*) $\zeta_0 = \eta_0 = 0$. $\kappa_0 = 0$. In this case there is no viscosity and heat conduction and our system of equations reduce to the Bianchi VI_0 perfect fluid models which have been studied by Collins (1971). We identify two cases: (1) $1 \le \gamma < 2$, (2) $\gamma = 2$. In case 1, we have four nondegenerate singular points. $(1, 0)$ is a saddle and $(0, -2)$ is a stable 2-tangent node. $(0, 2)$ is a degenerate singular point and the analysis shows that it must be of saddle type. Finally, the point $[1 - (3\gamma - 2)/4, (3\gamma - 2)/2]$ is an unstable focus. In case 2, each point on the boundary of $\mathscr{R}$ is a nonisolated singular

point. The point (0, 2) has an exceptional character such that all trajectories start from that point and terminate at a point on the boundary $\mathscr{R}$. The phase portraits are qualitatively the same as shown in Figs. 1 and 2, respectively.

$0 < \kappa_0 < 1$. If $1 \leq \gamma < 2$, (1, 0) is saddle. The point (0, 2) is a stable 2-tangent node (or stellar node). The point (0, −2) is a stable 2-tangent node. We define

$$\Psi = 1 - 9/4(3\gamma - 2) + (3\gamma - 2)^2/4(1 - \kappa_0{}^2)$$

$$\Phi = (3\gamma - 2) - 4(1 - \kappa_0{}^2)$$

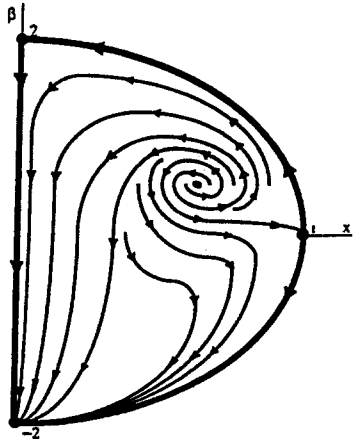

Fig. 1. The figures depict the evolution of a class of Bianchi VI_0 imperfect fluid models in terms of dimensionless variables x and β, defined by (2.16) and (2.17), respectively. The axes are drawn in the conventional sense (e.g., x increases from left to right), but the directions are marked, to prevent confusion with trajectories. Arrows refer to evolution in Ω-time ($\Omega \to +\infty$ indicates $t \to 0$, or approach to the singularity). This figure gives the phase portrait for the cases $\zeta_0 = \eta_0 = \kappa_0 = 0$ with $1 \leq \gamma < 2$ and $\zeta_0 = \eta_0 = 0$ with $0 < \kappa_0 < 1$, which are qualitatively the same.

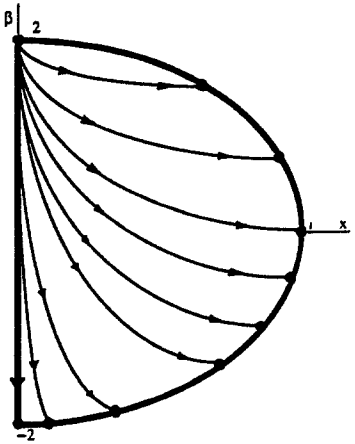

Fig. 2. Phase portrait corresponding to a perfect fluid with $\gamma = 2$.

Now, if $\Phi > 0$, the point F given by $[1-(3\gamma-2)/4(1-\kappa_0{}^2), (3\gamma-2)/2(1-\kappa_0{}^2)^{1/2}]$ occurs inside the region $\mathscr{R}$ as a nondegenerate singular point. There is also the singular point S $(0, 2(1-\kappa_0{}^2)^{1/2})$. If $\Phi < 0$, then point S is a saddle. Now, if $\Psi > 0$, then F is an unstable 2-tangent node (see Fig. 3). If $\Psi < 0$, then F is an unstable focus (see Fig. 1) and if $\Psi = 0$, then F would be an unstable stellar node. If $\Phi > 0$, then the point F is not inside $\mathscr{R}$ and the point S is an unstable 2-tangent node. If $\Phi = 0$, then F coincides with S and S is a degenerate singular point which turns out to be of unstable 2-tangent-node type. The phase portrait is qualitatively the same as that given in Fig. 4. If $\gamma = 2$, the boundary of $\mathscr{R}$ is a set of nonisolated singular points (see Fig. 5).

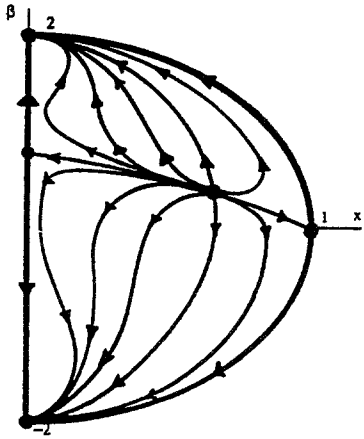

Fig. 3. The phase portrait for the cases $\zeta_0 = \eta_0 = 0$ with $0 < \kappa_0 < 1$, where $\Psi \geq 0$ and $\Phi < 0$, and $m = n = 1/2, 1, 3/2$, $0 < \kappa_0 < 1$, where $9\zeta_0 < 3\gamma - 2$, which are qualitatively the same.

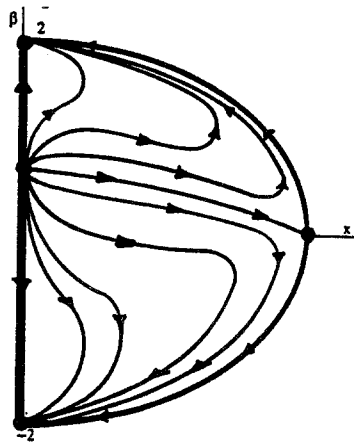

Fig. 4. The qualitative behavior of the following cases: $\zeta_0 = \eta_0 = 0$ with $0 < \kappa_0 \leq 1$ where $\Phi \geq 0$ and $1 \leq \gamma < 2$; $m = n = 1$, $0 < \kappa_0 < 1$, with $9\zeta_0 < 3\gamma - 2$; and $m = n = 3/2$, $0 < \kappa_0 \leq 1$, with $9\zeta_0 \leq 3\gamma - 2$.

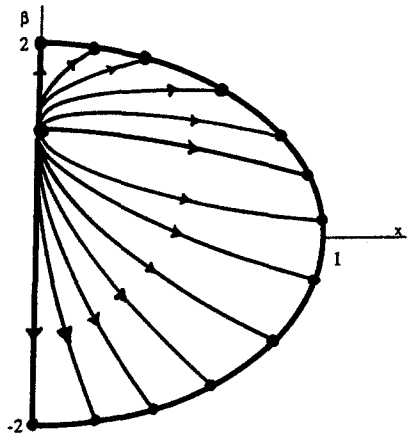

Fig. 5. The qualitative behavior of the model with perfect fluid and heat conduction, where $\gamma = 2$.

$\kappa_0 = 1$. This is an exceptional case in which there is heat conduction, but the corresponding plane-autonomous system takes a simpler form. There are four isolated singular points. If $1 \leq \gamma < 4/3$, then $(0, 0)$ is an unstable 2-tangent node. $(1, 0)$ is a saddle with separatrices $\beta = 0$ and $x = 1$. $(0, 2)$ is a stable 2-tangent node. $(0, -2)$ is also a stable 2-tangent node. If $\gamma = 4/3$, the point $(0, 0)$ becomes an unstable stellar node, because the two eigenvalues are equal. The remaining points still have the same character. If $4/3 < \gamma < 2$, the situation is exactly the same as $1 \leq \gamma < 4/3$ except that $x = 0$ is the main eigendirection for the point $(0, 0)$. If $\gamma = 2$, the boundary of $\mathscr{R}$ is a set of nonisolated singular points. The only isolated singular point is $(0, 0)$, which is an unstable 2-tangent node. The phase portraits are qualitatively the same as given in Fig. 4 for $\gamma \neq 2$ and Fig. 5 for $\gamma = 2$.

(b) $m = n = 0$. $0 \leq \kappa_0 < 1$. In this case, if $9\zeta_0 < 3\gamma - 2$, the point $(1, 0)$ is a saddle and another singular point $(\bar{x}, \bar{\beta})$ exists, where $\bar{\beta} > 0$. After investigation, this point is established to be a source. If $9\zeta_0 > 3\gamma - 2$, only the point $(1, 0)$ is singular and it is an unstable 2-tangent node. If $9\zeta_0 = 3\gamma - 2$, the point $(1, 0)$ is degenerate. By changing to polar coordinates and analyzing the signs of $\dot{r}$ and $\dot{\theta}$ close to the origin we find that $(1, 0)$ is of unstable 2-tangent-node type. The phase portraits are qualitatively the same as those sketched in Figs. 6 and 7, respectively.

$\kappa_0 = 1$. When $m = n = 0$ the β axis is not a solution of the system, so that trajectories may intersect the β axis, and (almost all) trajectories violate the weak energy conditions for finite time. This case is of two types, depending on whether ζ_0 is zero or not. If $\zeta_0 = 0$, then there are two

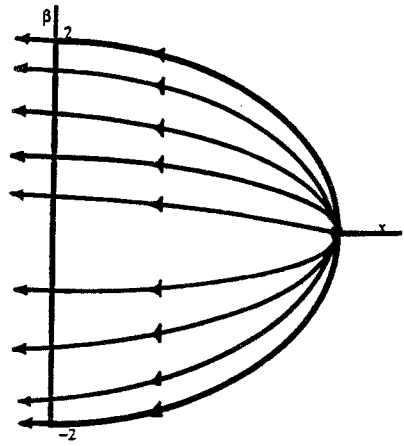

Fig. 6. The case $m = n = 0$ and $0 \leq \kappa_0 \leq 1$ with $9\zeta_0 \geq 3\gamma - 2$.

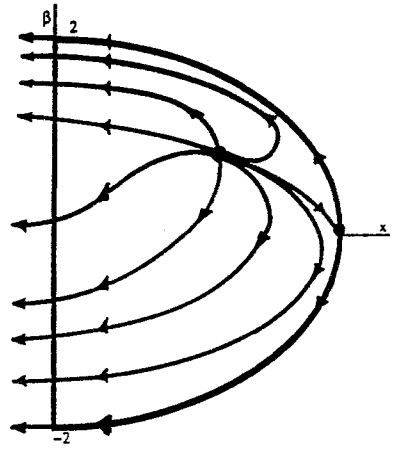

Fig. 7. The case $0 \leq \kappa_0 \leq 1$ with $9\zeta_0 < 3\gamma - 2$.

singular points. (1, 0) is a saddle and the point (0, 0) is an unstable 2-tangent node (see Fig. 8). If $\zeta_0 \neq 0$ and $9\zeta_0 < 3\gamma - 2$, then (1, 0) is a saddle. $(\Sigma, 0)$ with $\Sigma = 9\zeta_0/(3\gamma - 2)$ is an unstable 2-tangent node (see Fig. 7). If $9\zeta_0 > 3\gamma - 2$, the only singular point is (1, 0), which is an unstable 2-tangent node. Finally, if $9\zeta_0 = 3\gamma - 2$, the only singular point is (1, 0), which is degenerate, and analysis shows that it is of unstable-node type (see Fig. 6 for the phase portraits).

(c) $m = n = 1/2$. $\kappa_0 = 1$. In this case there are singular points (0, 0), (0, 2), (0, −2). The corresponding system is not analytic at these points, but by transforming to a new variable u and a new time coordinate τ

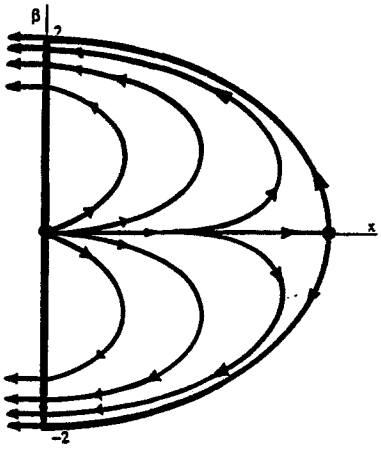

Fig. 8. The case where $m = n = 0$, $\kappa_0 = 1$, and $\zeta_0 = 0$.

($u^2 = x$; $d\Omega/d\tau = u$), we find that all three singular points are degenerate. At (0, 0), in the region of interest there are invariant rays $\theta = 0$, $\pi/2$, and $3\pi/2$. By analyzing the signs of $\dot{r}$ and $\dot{\theta}$ we find that the first and fourth quadrants are hyperbolic sectors. At $(0, -2)$ there are invariant rays $\theta = 0$ and $\pi/4$. The boundary of $\mathscr{R}$ is represented by $\beta^2 + 4u^2 = 4$, so the invariant ray $\theta = 0$ corresponds to the trajectory along the boundary of $\mathscr{R}$. Analysis shows that the two points (0, 2) and $(0, -2)$ are both of stable-node type. There is a fourth singular point (1, 0). When $9\zeta_0 < 3\gamma - 2$, (1, 0) is a saddle and a fifth point $(\Sigma, 0)$ occurs where $\Sigma = [9\zeta_0/(3\gamma - 2)]^2$. It is an unstable 2-tangent node (see Fig. 3). If $9\zeta_0 > 3\gamma - 2$, (1, 0) is an unstable 2-tangent node. When $9\zeta_0 = 3\gamma - 2$, (1, 0) is a degenerate point which has the character of two hyperbolic sectors. The phase portrait is qualitatively the same as given in Fig. 9.

$0 < \kappa_0 < 1$. In this case, there are singular points (1, 0), (0, 2), $(0, -2)$, $(\Sigma, 0)$, and $(0, 2[1 - \kappa_0^2]^{1/2})$. The points (0, 2) and $(0, -2)$ are degenerate singular points, and standard analysis shows that they are of stable-node type. The point $(0, 2[1 - \kappa_0^2]^{1/2})$ is a degenerate singular point which consists of two hyperbolic sectors. If $9\zeta_0 < 3\gamma - 2$, then the point (1, 0) is a saddle. In this case an interior point $(\bar{x}, \bar{\beta})$ occurs and is a source. If $9\zeta_0 > 3\gamma - 2$, (1, 0) is an unstable 2-tangent node with the same eigendirections. If $9\zeta_0 = 3\gamma - 2$, then the point (1, 0) is of unstable degenerate node type. The phase portraits are qualitatively the same as the case $\kappa_0 = 1$.

$\kappa_0 = 0$. In this case $(0, 2[1 - \kappa_0^2]^{1/2})$ coincides with (0, 2) and is degenerate. Analysis of $\dot{r}$ and $\dot{\theta}$ near (0, 2) shows that the region between $x = 0$ and $\theta = -\pi/4$ is a hyperbolic sector. Again if $9\zeta_0 < 3\gamma - 2$, then (1, 0) is a saddle and there exists a source $(\bar{x}, \bar{\beta})$ where $\bar{\beta} > 0$ (see Fig. 11).

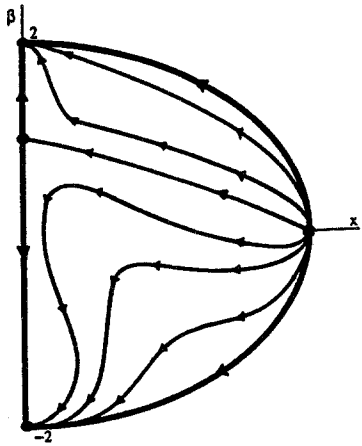

Fig. 9. The qualitative behavior of the following cases: $m = n = 1/2$, $0 < \kappa_0 \leq 1$ with $9\zeta_0 \geq 3\gamma - 2$; $m = n = 1$, $0 < \kappa_0 \leq 1$, and $m = n = 3/2$, $0 < \kappa_0 < 1$, with $9\zeta_0 > 3\gamma - 2$.

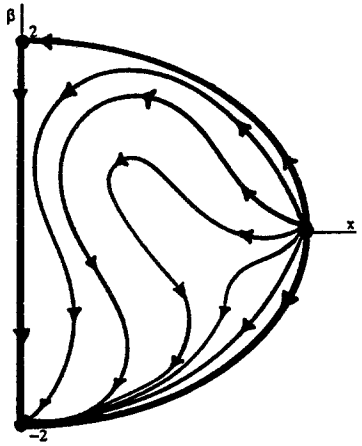

Fig. 10. Phase portrait corresponding to the case $m = n = 1, 3/2$, $\kappa_0 = 0$, with $9\zeta_0 \geq 3\gamma - 2$.

If $9\zeta_0 \geq 3\gamma - 2$, then $(1, 0)$ is an unstable 2-tangent node. The phase portrait is sketched in Fig. 10.

(d) $m = n = 1$. $\kappa_0 = 1$. If $9\zeta_0 < 3\gamma - 2$, the singular point $(0, 0)$ is an unstable 2-tangent node. The point $(1, 0)$ is a saddle with separatrices $x = 1$ and $\beta = 0$ (see Fig. 4). If $9\zeta_0 > 3\gamma - 2$, then $(0, 0)$ is a saddle, and $(1, 0)$ becomes an unstable 2-tangent node. The points $(0, 2)$ and $(0, -2)$ in all cases are stable 2-tangent nodes (see Fig. 9). If $3\gamma - 2 - 9\zeta_0 = 0$, each point $(x, 0)$ for $0 \leq x \leq 1$ is a singular point, i.e., the x axis is a line singularity. Calculating the slope of the trajectories as $\beta \to 0$, we obtain $d\beta/dx \to \infty$,

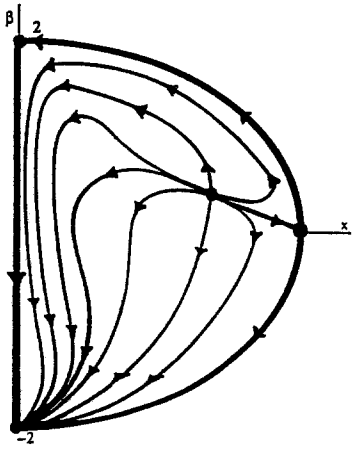

Fig. 11. Phase portrait for the case $m = n = 1, 3/2$, $\kappa_0 = 0$, with $9\zeta_0 < 3\gamma - 2$.

i.e., the trajectories are perpendicular to the x axis. The phase portrait is given in Fig. 12.

$0 < \kappa_0 < 1$. The points $(0, 2)$ and $(0, -2)$ are stable 2-tangent nodes. Now, if $9\zeta_0 < 3\gamma - 2$ and $\Delta < 0$, where

$$\Delta = 3\gamma - 2 - 9\zeta_0 - (12\eta_0 + 4)(1 - \kappa_0{}^2)$$

then the singular point $(0, 2[1 - \kappa_0{}^2]^{1/2})$ is a saddle. In this case another singular point $(\bar{x}, \bar{\beta})$ occurs, which calculation shows to be a source. In addition, the singular point $(1, 0)$ is a saddle (see Fig. 3). If $\Delta \geq 0$, the point

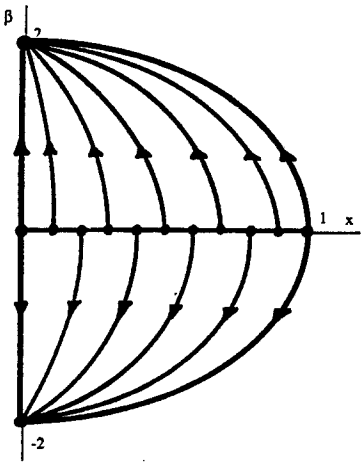

Fig. 12. The phase portrait for the case $m = n = 1$, $\kappa_0 = 1$ with $9\zeta_0 = 3\gamma - 2$.

$(0, 2[1-\kappa_0{}^2]^{1/2})$ is an unstable 2-tangent node (see Fig. 4). If $9\zeta_0 > 3\gamma - 2$, the point $(1, 0)$ is an unstable 2-tangent node. The point $(0, 2[1-\kappa_0{}^2]^{1/2})$ becomes a saddle with the same separatrices as before. If $9\zeta_0 = 3\gamma - 2$, the only singular point is $(1, 0)$, which an analysis of the sign of $\dot{r}$ and $\dot{\theta}$ shows to be of unstable 2-tangent-node type. The phase portrait is qualitatively the same as shown in Fig. 9.

$\kappa_0 = 0$. In this case the point $(0, 2[1-\kappa_0{}^2]^{1/2})$ coincides with $(0, 2)$ and Δ is always positive. $(0, 2)$ is a degenerate singular point, which standard analysis shows to be of saddle type with $x = 0$ and $\beta + x - 2 = 0$ as separatrices. The various possibilities, depending on the sign of $3\gamma - 2 - 9\zeta_0$, are the same as the previous case (i.e., $m = n = 1/2$, $\kappa_0 = 0$).

(e) $m = n = 3/2$. $\kappa_0 = 1$. If $\gamma \neq 2$, there are singular points $(0, 0)$, $(1, 0)$, $(0, 2)$, and $(0, -2)$. The point $(0, 0)$ is an unstable 2-tangent node. If $\gamma = 4/3$, then the origin is an unstable stellar node. The points $(0, 2)$ and $(0, -2)$ are stable 2-tangent nodes. The rest of the analysis depends on the sign of $3\gamma - 2 - 9\zeta_0$. If $9\zeta_0 > 3\gamma - 2$, then there are two further singular points; $(1, 0)$ is an unstable 2-tangent node and there is a saddle at $(\Sigma, 0)$, where $\Sigma = [(3\gamma - 2)/9\zeta_0]^{1/2}$ (see Fig. 13). If $9\zeta_0 < 3\gamma - 2$, then $(1, 0)$ is a saddle. If $9\zeta_0 = 3\gamma - 2$, then $(1, 0)$ is degenerate, which calculation shows to be a saddle. [In this latter case the point $(\Sigma, 0)$ coincides with $(1, 0)$.] If $\gamma = 2$, the points $(0, 2)$ and $(0, -2)$ are degenerate. Standard calculation shows them to be stable 2-tangent nodes. The remainder of the analysis is same as in the case $\gamma \neq 2$. The phase portrait is qualitatively the same as that given in Fig. 4.

$0 < \kappa_0 < 1$. $\gamma \neq 2$. The points $(0, 2)$ and $(0, -2)$ are stable 2-tangent nodes. If $9\zeta_0 < 3\gamma - 2$, then $(1, 0)$ is a saddle. If $3\gamma - 2 < 4(1 - \kappa_0{}^2)$, then

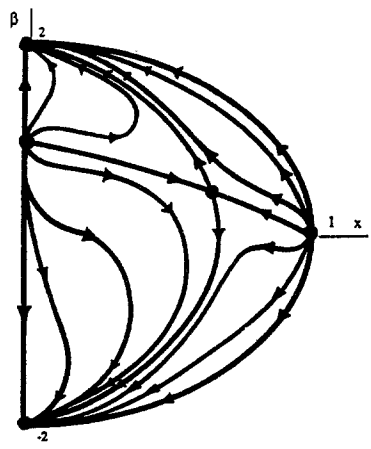

Fig. 13. The qualitative behavior of the case $m = n = 3/2$, $0 < \kappa_0 < 1$, where $9\zeta_0 > 3\gamma - 2$ and $3\gamma - 2 > 4(1 - \kappa_0{}^2)$.

the point $(0, 2[1-\kappa_0^2]^{1/2})$ is a singular saddle point. In this case another singular point $(\bar{x}, \bar{\beta})$ in the interior of $\mathscr{R}$ occurs which calculation shows to be a source (see Fig. 3). If $3\gamma - 2 > 4(1-\kappa_0^2)$, the point $(0, 2[1-\kappa_0^2]^{1/2})$ is an unstable 2-tangent node (see Fig. 4). If $3\gamma - 2 = 4(1-\kappa_0^2)$, then the point $(0, 2[1-\kappa_0^2]^{1/2})$ is a degenerate singular point which analysis shows to be of unstable-node type. The phase portrait related to this case is similar to the case $3\gamma - 2 > 4(1-\kappa_0^2)$. Finally, if $9\zeta_0 > 3\gamma - 2$, then $(1, 0)$ is an unstable 2-tangent node. If $3\gamma - 2 > 4(1-\kappa_0^2)$, then the point $(0, 2[1-\kappa_0^2]^{1/2})$ is an unstable 2-tangent node (see Fig. 13). In this case another singular point $(\bar{x}, \bar{\beta})$ occurs in the interior of $\mathscr{R}$, which is a saddle. If $9\zeta_0 < 3\gamma - 2$, then the point $(0, 2[1-\kappa_0^2]^{1/2})$ is a saddle. The phase portrait is qualitatively the same as that given in Fig. 9.

$\kappa_0 = 0$. In this case the point $(0, 2[1-\kappa_0^2]^{1/2})$ coincides with the point $(0, 2)$. Now $(0, 2)$ is a degenerate singular point which is of saddle type. If $9\zeta_0 < 3\gamma - 2$, then $(1, 0)$ is a saddle and there is an interior singular point which is a source. If $9\zeta_0 \geq 3\gamma - 2$, then $(1, 0)$ is an unstable 2-tangent node and, as before, $(0, 2)$ is a stable 2-tangent node. The phase portraits in this case are qualitatively the same as the case $m = n = 1/2$ with $\kappa_0 = 0$.

Moreover, the investigation shows that all cases $m = n > 1$ are qualitatively the same as the case $m = n = 3/2$ studied here.

5. ENERGY CONDITIONS

The energy-momentum tensor satisfies certain physical inequalities.

(i) *The weak energy condition* (WEC):

$$-\lambda_0 \geq 0, \qquad -\lambda_0 + \lambda_\alpha \geq 0 \quad (\alpha = 1, 2, 3) \tag{5.1a}$$

where λ_0 corresponds to the eigenvalue associated with the timelike eigenvector and λ_α are the eigenvalues associated with the eigenvectors of T_{ab}.

(ii) *The dominant energy condition* (DEC):

$$-\lambda_0 \geq 0, \qquad \lambda_0 \leq \lambda_\alpha \leq -\lambda_0 \tag{5.1b}$$

(iii) *The strong energy condition* (SEC):

$$-\lambda_0 + \sum_{\mu=1}^{3} \lambda_\mu \geq 0, \qquad -\lambda_0 + \lambda_\alpha \geq 0 \tag{5.1c}$$

We note that care must be taken in checking these energy conditions in situations, similar to those under consideration here, in which the energy-momentum tensor is not diagonal.

The eigenvalues of the Bianchi VI_0 imperfect fluid energy-momentum tensor given by equation (2.2) are given by

$$\begin{aligned}
\frac{\lambda_0}{\theta^2} &= \frac{1}{2}\left[-\frac{1}{3}x + \frac{1}{3}(\gamma-1)x - \zeta_0 x^m - \frac{2}{3}\beta\eta_0 x^n(1-\kappa_0^2)^{1/2} + \sqrt{\Delta}\right] \\
\frac{\lambda_1}{\theta^2} &= \frac{1}{2}\left[-\frac{1}{3}x + \frac{1}{3}(\gamma-1)x - \zeta_0 x^m - \frac{2}{3}\beta\eta_0 x^n(1-\kappa_0^2)^{1/2} - \sqrt{\Delta}\right] \qquad (5.2) \\
\frac{\lambda_2}{\theta^2} &= \frac{\lambda_3}{\theta^2} = \frac{1}{3}(\gamma-1)x - \zeta_0 x^m + \eta_0 x^n\left[\frac{1}{\sqrt{3}}\kappa_0\beta + \frac{1}{3}\beta(1-\kappa_0^2)^{1/2}\right]
\end{aligned}$$

where

$$\Delta = \left[-\frac{1}{3}x - \frac{1}{3}(\gamma-1)x + \zeta_0 x^m + \frac{2}{3}\eta_0\beta x^n(1-\kappa_0^2)^{1/2}\right]^2 + \frac{4\kappa_0^2\beta^2}{3\theta^2}$$

Now, a given model, with specific values for ζ_0, η_0, κ_0, m, n, and γ, may or may not satisfy the weak and dominant and/or strong energy conditions for all x and β. Because of the complexity of the eigenvalues, a full analysis of the energy conditions is difficult. But a full analysis can be achieved if we concern ourselves with the special case $\kappa_0 = 0$ (i.e., no heat conduction), where the energy-momentum tensor is diagonal. As an illustration, let us then consider this case in detail. By continuity, all results here would follow in the neighborhood of $\kappa_0 = 0$ (i.e., for small κ_0). In this case, the eigenvalues are given by

$$\begin{aligned}
\frac{\lambda_0}{\theta^2} &= -\frac{1}{3}x \\
\frac{\lambda_1}{\theta^2} &= \frac{1}{3}(\gamma-1)x - \zeta_0 x^m - \frac{2}{3}\eta_0\beta x^n \qquad (5.3) \\
\frac{\lambda_2}{\theta^2} &= \frac{\lambda_3}{\theta^2} = \frac{1}{3}(\gamma-1)x - \zeta_0 x^m + \frac{1}{3}\eta_0\beta x^n
\end{aligned}$$

The inequality $-\lambda_0 \geq 0$ implies that $x \geq 0$. Any trajectory that crosses the β axis must have x, and thus ρ, negative after (or before) a finite time. Such models can only be physically realistic for certain time periods. The only case in which trajectories can cross the β axis is when $m = n = 0$, whence the WEC is violated.

The remaining conditions of the WEC lead to

$$\frac{1}{3}\gamma x - \zeta_0 x^m - \frac{2}{3}\eta_0\beta x^n \geq 0 \qquad (5.4a)$$

$$\frac{1}{3}\gamma x - \zeta_0 x^m + \frac{1}{3}\eta_0\beta x^n \geq 0 \qquad (5.4b)$$

In order to obtain a sufficient condition for (5.4a) to be satisfied for all β and x we put $\beta = 2$ (its maximum value), so that

$$\frac{1}{3}\gamma x - \zeta_0 x^m - \frac{4}{3}\eta_0 x^n \geq 0 \tag{5.5}$$

We will return to this inequality and discuss conditions under which it is satisfied for different values of $m = n$. We see that (5.5) is a sufficient condition for (5.4b) to be satisfied. The DEC leads to

$$\frac{1}{3}(2-\gamma)x + \zeta_0 x^m + \frac{2}{3}\beta\eta_0 x^n \geq 0 \tag{5.6a}$$

$$\frac{1}{3}(2-\gamma)x + \zeta_0 x^m - \frac{1}{3}\beta\eta_0 x^n \geq 0 \tag{5.6b}$$

A simple analysis shows that the condition

$$\zeta_0 - \frac{4}{3}\eta_0 \geq 0 \tag{5.7}$$

in addition to the WEC, is a sufficient condition for the DEC to be satisfied for all x and β and $m = n$. Finally, the SEC implies that

$$\left(\gamma - \frac{2}{3}\right)x - 3\zeta_0 x^m \geq 0 \tag{5.8}$$

in addition to the WEC.

Now, let us discuss the conditions to be met in order for the energy conditions (5.5) and (5.8) to be satisfied. For the perfect fluid case (when $\zeta_0 = \eta_0 = 0$), all energy conditions are met. When $m = n = 0$, the WEC can be satisfied for those parts of the trajectories with $x \geq (3\zeta_0 + 4\eta_0)/\gamma$, where $\gamma - 3\zeta_0 - 4\eta_0 \geq 0$, else there are no values of x in $\mathscr{R}$ such that the energy conditions are met. The SEC can be satisfied for $x \geq 9\zeta_0/(3\gamma - 2)$, where $3\gamma - 2 \geq 9\zeta_0$ (in order to keep $x \leq 1$). When $m = n = 1/2$, then the WEC can be satisfied for those parts of the trajectories with $x \geq [(3\zeta_0 + 4\eta_0)/\gamma]^2$, where $\gamma - 3\zeta_0 - 4\eta_0 \geq 0$. The SEC can be met for $x \geq [9\zeta_0/(3\gamma - 2)]^2$, where $3\gamma - 2 \geq 9\zeta_0$. For $0 < m(=n) < 1$, similar conditions exist for the satisfaction of the WEC and SEC, and the energy conditions can be met for $x > 0$. However, the WEC and SEC can never be met in this case for x close to 0. When $m = n = 1$, the WEC is satisfied for all trajectories in $\mathscr{R}$ provided $\gamma - 3\zeta_0 - 4\eta_0 \geq 0$, and the SEC will be met if $3\gamma - 2 \geq 9\zeta_0$. For example, in this case with $\gamma = 3/2$, $\zeta_0 = 1/6$, and $\eta_0 = 1/12$, all the energy conditions are met.

When $m = n = 3/2$, those parts of the trajectories with $x \leq [\gamma/(3\zeta_0 + 4\eta_0)]^2$, where $\gamma - 3\zeta_0 - 4\eta_0 \geq 0$, satisfy the WEC, and those with

$x \leq [(3\gamma - 2)/9\zeta_0]^2$, where $3\gamma - 2 \geq 9\zeta_0$, satisfy the SEC. Clearly there are value of the parameters for which the energy conditions are met for all trajectories in $\mathscr{R}$. This is the situation in all cases with $m, n = 1$. The condition $3\zeta_0 - 4\eta_0 \geq 0$ is a sufficient condition for the DEC to be satisfied for all cases.

In Figs. 6–8 (corresponding to the case $m = n = 0$, $0 \leq \kappa_0 \leq 1$), the WEC cannot be satisfied close to the β axis (i.e., $x \approx 0$). The SEC can never be satisfied in Fig. 8 and cannot be satisfied for $x \approx 0$ in Fig. 6. In Figs. 10 and 11 (corresponding to the case $m = n = 1/2$, $\kappa_0 = 0$), the WEC cannot be satisfied for those parts of the trajectories in which $x \approx 0$ and the SEC cannot be met in Fig. 10 when $x \approx 0$ and in Fig. 11 for all trajectories in $\mathscr{R}$. In Figs. 10 and 11 (corresponding to the case $m = n = 1$, $\kappa_0 = 0$), the WEC is satisfied provided $\gamma - 3\zeta_0 - 4\eta_0 \geq 0$, and the SEC is satisfied only in Fig. 10 where $9\zeta_0 < 3\gamma - 2$.

6. DISCUSSION

By using geometric techniques of the theory of differential equations, we have been able to determine the precise qualitative behavior of a class of Bianchi VI_0 imperfect fluid models with equations of state (3.1). The global behavior depends mainly on the bulk viscosity, although the precise local details depend on both the bulk and shear viscosity. We have found that a variety of possibilities exist. From the derived dynamical system we have been able to calculate the asymptotic behavior of models both to the past and future.

Certain phase portraits for Bianchi VI_0 (BVI_0) models, in which viscosity and heat conduction have been included, are remarkably similar to those in the Bianchi V (BV) case (Coley and Dunn, 1992). The case $\zeta_0 = \eta_0 = 0$, $\kappa_0 = 1$ is qualitatively the same as in the BV perfect fluid case. When $0 < \kappa_0 < 1$, the points $(1, 0)$ and $(0, -2)$ have the same character in both types. When $m = n = 0$ and $\kappa_0 = 1$, the phase portraits in both types are qualitatively the same, although the phase portraits are no longer symmetric about the x-axis in type VI_0. In the case $m = n = 1$ and $\kappa_0 = 1$, when $9\zeta_0 < 3\gamma - 2$, the phase portrait is the same as that for the BV perfect fluid with $1 \leq \gamma < 2$.

We note that in the BV case the trajectories are not symmetric about the x axis, except in the perfect fluid case, while in type VI_0 models, all cases with $\kappa_0 = 1$ are symmetric about the x axis. In the type V case the trajectories cannot intersect the x axis, but all trajectories in the cases with $0 \leq \kappa_0 < 1$ here cross the x axis. In the BV case, $x = 0$ is not always a solution of the plane-autonomous system of type BV (i.e., some trajectories intersect the β axis and consequently violate the WEC). However, in type

BVI_0, $x = 0$ is itself a trajectory (unless $m = n = 0$), whence no other trajectories can intersect it. In all cases (unless $m = n = 0$) when $\kappa_0 = 0$, the point (0, 2) is a saddle, unlike in the BV case.

In the Bianchi type VI_0 perfect fluid case, when $1 \leq \gamma < 2$, a focus occurs, but in the presence of dissipation this feature always disappears. Moreover, the extra singular points (0, 0) or $(0, 2[1 - \kappa_0^2]^{1/2})$ appear when viscosity and heat condition are taken into account. In the perfect fluid case, the points (1, 0), (0, 2), and $(\bar{x}, \bar{\beta})$ correspond to a saddle, saddle, and focus, respectively, but in the presence of viscosity and heat conduction the role of these points may change; for example, (1, 0) may become an unstable node and (0, 2) a stable node. Indeed, the effect of viscosity and heat conduction produce many different possible phase portraits, unlike the unique picture in the perfect fluid case.

In contrast to earlier work (Coley and Dunn, 1992; Belinskii and Khalatnikov, 1976), we have included heat conduction in a general way. The quantity q_1 appears in our plane-autonomous system, so that it is necessary to extend the set of "dimensionless equations of state" to incorporate a dimensionless equation of state for q_1 in order to keep the system two-dimensional and autonomous. This equation of state includes an adjustable parameter κ_0 such that heat conduction can be "turned off." In the absence of heat conduction ($\kappa_0 = 0$) the cases $m = n = 1, 1/2, 3/2$ have the same qualitative behavior.

The singular point $(0, 2[1 - \kappa_0^2]^{1/2})$ approaches the point (0, 2) as $\kappa_0 \to 0$; when $\kappa_0 = 0$, the two points coincide and (when $m = n = 1/2, 1, 3/2$) the singular point (0, 2) is of degenerate saddle type. This can never happen in the corresponding BV models.

Finally, let us consider the exact solutions corresponding to the various singular points. The singular points that occur on the boundary $\beta^2 + 4x = 4$ correspond to Bianchi I solutions, which are well known (Collins, 1971). Let a singular point be denoted by $(\tilde{x}, \tilde{\beta})$, where $\tilde{x}$ and $\tilde{\beta}$ are constants satisfying $\tilde{\beta}^2 + 4\tilde{x} < 4$. From equation (2.12) we find that

$$X(t)\theta(t) = 2\sqrt{3}(4 - \tilde{\beta}^2 - 4\tilde{x})^{-1/2} \tag{6.1}$$

It then follows from equations (2.5), (2.9), and (2.10) that $\dot{X}X^{-1}$, $\dot{Y}Y^{-1}$, and $\dot{Z}Z^{-1}$ are all proportional to θ, and that (after rescaling) the corresponding exact solutions are of the form

$$X(t) = at, \qquad Y(t) = t^b, \qquad Z(t) = t^c \tag{6.2}$$

where a, b, and c are constants.

In the cases of the singular points $(0, \tilde{\beta})$ and $(\tilde{x}, 0)$, with $\rho\theta^{-2} = 0$ and $\sigma\theta^{-1} = 0$, it is found that there are no (corresponding) consistent exact solutions of the Einstein field equations of the form (6.2) with $\rho = 0$ and

$\sigma = 0$, respectively. In the remaining case ($\tilde{x}, \tilde{\beta}$; $\tilde{x}^2 + \tilde{\beta}^2 \neq 0$) there do indeed exist exact solutions of the form (6.2), where the various constants satisfy the following algebraic relations:

$$\begin{aligned} a &= \frac{2}{\sqrt{3}}(1 + \tilde{\beta}\delta)(4 - \tilde{\beta}^2 - 4\tilde{x})^{-1/2} \\ b &= \left(1 - \frac{\sqrt{3}}{2}\kappa_0\tilde{\beta} - \frac{1}{2}\tilde{\beta}\delta\right)(1 + \tilde{\beta}\delta)^{-1} \\ c &= \left(1 + \frac{\sqrt{3}}{2}\kappa_0\tilde{\beta} - \frac{1}{2}\tilde{\beta}\delta\right)(1 + \tilde{\beta}\delta)^{-1} \end{aligned} \tag{6.3}$$

where $\delta = (1 - \kappa_0^2)^{1/2}$ and $\tilde{x}$ and $\tilde{\beta}$ satisfy equations (3.2) and (3.3) with $x' = \beta' = 0$ in terms of γ, η_0, ζ_0, and κ_0 (and m and n); e.g., for $m = n = 1$ we have that

$$\begin{aligned} \tilde{x} &= 1 - \frac{1 + 3\eta_0}{\kappa_0 - 9\zeta_0}\tilde{\beta}^2 \\ \tilde{\beta} &= \frac{\delta}{3\eta_0}\{-1 \pm [1 + 3\eta_0(3\gamma - 2 - 9\zeta_0)^{-2}]^{1/2}\} \end{aligned} \tag{6.4}$$

where $3\gamma - 9\zeta_0 - 2 > 0$ and

$$[\delta + 3\eta_0(\kappa_0 - 9\zeta_0)]^{1/2} \leq 3\eta_0(\kappa_0 - 9\zeta_0)^{1/2}(1 + 3\eta_0)^{-1/2} + \delta$$

in order for $(\tilde{x}, \tilde{\beta})$ to be in $\mathscr{R}$.

ACKNOWLEDGMENTS

This work was supported in part by the Natural Sciences and Engineering Research Council of Canada.

REFERENCES

Belinskii, V. A., and Khalatnikov, I. M. (1976). *Soviet Physics-JETP*, **42**, 205.
Bradley, J. M., and Sviestins, E. (1984). *General Relativity and Gravitation*, **16**, 1119.
Coley, A. A. (1990*a*). *General Relativity and Gravitation*, **22**, 3.
Coley, A. A. (1990*b*). *Journal of Mathematical Physics*, **31**, 1698.
Coley, A. A., and Dunn, K. A. (1992). *Journal of Mathematical Physics*, **33**, 1772.
Collins, C. B. (1971). *Communications in Mathematical Physics*, **23**, 137.
Misner, C. W. (1968). *Astrophysics Journal*, **151**, 431.